Shot-domain 4D time-lapse velocity analysis using apparent image displacements

Francesco Perrone and Paul Sava, Center for Wave Phenomena, Colorado School of Mines*

SUMMARY

Hydrocarbon production modifies the stress conditions in the subsurface and changes the model parameters previously estimated from the prospect. The capability to remotely monitor the changes in the reservoir using seismic data has strategic importance since it allows us to infer fluid movement and evolution of stress conditions, which are key factors to enhance recovery and reduce uncertainty and risk during production. A model of the subsurface parameters is necessary to reconstruct the seismic waves traveling through the medium and thus correctly image reflectors in the subsurface. Geomechanical changes in the subsurface can be measured by changes of seismic images obtained from the recorded data of multiple time-lapse surveys. We estimate changes of subsurface model parameters using the apparent shifts between migrated images obtained by 4D time-lapse seismic surveys. The apparent shifts are measured using penalized local correlations in the image domain, and they are exploited using wavefield tomography with an objective function minimized using the adjoint-state method. Our time-lapse monitoring method is efficient due to the fact that inversion can be conducted for pairs of seismic experiments, which eliminates the need to construct costly gathers. Since relatively small amounts of data are needed, our method can be used to invert for model changes at short intervals, thus increasing the resolution of 4D monitoring.

INTRODUCTION

Production of a hydrocarbon reservoir changes the physical parameters of the subsurface. Oil and/or gas extraction modifies the bulk modulus of the rocks and affects the geomechanics of the area. Stress changes induced by hydrocarbon production represent a key issue for constructing a geomechanical model of the reservoir. Monitoring these changes using remote sensing techniques, e.g., by seismic reflection data, is crucial for the oil and gas industry to design wells, predict recovery, and mitigate hazards and risk (Lumley, 2001).

Seismic waves are sensitive to the elastic properties of the subsurface. The propagation velocities of the elastic waves are directly related to to the stress state in the subsurface (Aki and Richards, 2002). By repeated seismic surveys over a reservoir at the various production stages, we can track changes in the propagation velocity in the subsurface and reconstruct the perturbation with respect to an initial model. This analysis exploits the sensitivity of the seismic waves to the elastic parameters of the subsurface. Inversion maps the changes in the recorded waveforms into a perturbation of the velocity model, which can then be related to stresses in the subsurface for geomechanical applications.

Time-lapse analysis is usually performed in the time domain (Hatchell and Bourne, 2005) and assumes small perturbations with respect to the background (baseline) model. Great care must be taken to match the baseline and monitor survey, a process called cross-equalization (Rickett and Lumley, 2001), in order to remove from the data all the differences that are not related to changes in the model parameters (e.g., differences in acquisition geometry). Similarly, time-lapse analysis can be done in the image domain, which is less sensitive to differences in the acquisition geometries and thus more robust against repeatability issues than the data domain.

Shragge and Lumley (2012) propose a linearized inversion approach in the depth-domain based on the wave-equation migration velocity analysis algorithm developed by Sava and Biondi (2004). Shragge et al. (2012) apply the methodology developed by Yang and Sava (2011) to 4D seismic monitoring and uses the adjoint-state method (Fichtner et al., 2006), which removes the linearity assumptions. By operating directly in the depth domain without linearity assumptions, this inversion can handle strong errors in the velocity model.

Wave-equation MVA (Sava and Biondi, 2004) and image-domain waveform tomography (Yang and Sava, 2011) require complete aperture to correctly construct the image perturbation that drives the tomographic procedure and to evaluate focusing in the subsurface, respectively. The requirements for the acquisition geometry can be relaxed using the approach proposed by Yang and Sava (2012); nonetheless, a large aperture is necessary for resolution purposes. We advocate the use of local image correlations (Hale, 2007) to measure the relative displacement between pairs of shot-migrated images and then use the inversion technique of Perrone and Sava (2012) to evaluate a model update following production. Local image correlations allow us to estimate the velocity model errors shot by shot. The image-domain approach is robust against repeatability issues, such as errors in the shot and receiver positions, and the adjoint-state method allows us to implement a nonlinear inversion procedure, which is effective for large and complex model updates. Furthermore, this technique does not require complete surveys for 4D monitoring , thus increasing its usability in areas with dense production infrastructure.

THEORY

Perrone and Sava (2012) restate the semblance principle considering locally coherent events in the image domain: the velocity model is correct when the images from different neighboring experiments show conformal features, that is, when the dips of the reflectors in two images are point-wise consistent. This criterium can be applied to migration velocity analysis using local image correlations to evaluate the relative movement of two images with respect to their structural dips. We can use the same idea for 4D time-lapse seismic and compare the images obtained from the baseline and monitor survey. We measure shifts of the monitor image with respect to the baseline, which represents the reference. The shift is measured along the normal to the reflector (in the dip direction). This shift is indicative of changes of the reservoir properties.

We set an optimization problem by defining the objective function

$$\mathcal{J}(m) = \frac{1}{2} \| \sum_{\boldsymbol{\lambda}} \mathcal{P}(\mathbf{x}, \boldsymbol{\lambda})\, c(\mathbf{x}, \boldsymbol{\lambda}) \|_{\mathbf{x}}^2, \qquad (1)$$

where $c(\mathbf{x}, \boldsymbol{\lambda}) = \int_{w(\mathbf{x})} R_{bsl}\left(\boldsymbol{\xi} - \frac{\boldsymbol{\lambda}}{2}\right) R_{mon}\left(\boldsymbol{\xi} + \frac{\boldsymbol{\lambda}}{2}\right) d\boldsymbol{\xi}$ is the local correlation of the baseline image $R_{bsl}(\mathbf{x})$ with the monitor image $R_{mon}(\mathbf{x})$, and $\mathcal{P}(\mathbf{x}, \boldsymbol{\lambda})$ is a penalty operator that highlights features which are related to velocity errors. The correlations are computed in local seamless overlapping windows $w(\mathbf{x})$, and the variable $m(\mathbf{x})$ denotes the model, which is slowness squared in our implementation to simplify the expression of the gradient of the objective function. When the velocity model is correct, the two images are perfectly aligned and the residual $\sum_{\boldsymbol{\lambda}} \mathcal{P}(\mathbf{x}, \boldsymbol{\lambda})\, c(\mathbf{x}, \boldsymbol{\lambda})$, a proxy for the relative displacement, is at minimum.

We assume that the shifts between the migrated baseline and monitor survey are related to the errors in the velocity model and that they are not physical movements of the reflectors due to subsidence; typically these movements can be in the order of a meter between the top and bottom of the reservoir (Hatchell and Bourne, 2005), and it is thus safe to assume that the estimated shifts in the reflector positions are due to changes in the migration model and not to changes of the positions of the interfaces. Nonetheless, this remains an assumption and future work will have to quantify its impact on the inverted models.

We compute the gradient of the objective function in equation 1 using the adjoint-state method (Fichtner et al., 2006; Plessix, 2006). The migrated images are defined as the zero-lag time-correlation of the source and receiver wavefield $u_s(\mathbf{x}, t)$ and $u_r(\mathbf{x}, t)$, which are extrapolated in a model $m(\mathbf{x})$ of the subsurface. The wavefields are computed by solving the wave-equations

$$\mathcal{L}(m)\, u_s = f_s,\ \mathcal{L}(m)\, u_r = f_r, \qquad (2)$$

where $\mathcal{L}(m) = m\, \partial_{tt} - \nabla^2$ is the d'Alambert operator, $f_s(\mathbf{x}_s, t)$ and $f_r(\mathbf{x}_r, t)$ are the source function and the reflected data, respectively, and $\mathbf{x}_s$ and $\mathbf{x}_r$ indicate the source and receiver positions. In this formulation, $m(\mathbf{x})$ represents slowness squared and, since $\mathcal{L}(m)$ is linear in m, this choice simplifies the expression of the gradient of the objective function (Fichtner et al., 2006). The gradient of the objective function is

$$\nabla_m \mathcal{J} = \int (\ddot{u_s} a_s + \ddot{u_r} a_r) dt, \qquad (3)$$

where the adjoint wavefields $a_s(\mathbf{x}, t)$ and $a_r(\mathbf{x}, t)$ are solutions to the wave-equations

$$\mathcal{L}^\dagger(m)\, a_s = g_s,\ \mathcal{L}^\dagger(m)\, a_r = g_r. \qquad (4)$$

$\mathcal{L}^\dagger(m)$ is the adjoint of the d'Alambert operator, and the adjoint sources $g_s(\mathbf{x}, t) = \nabla_{u_s} \mathcal{J}$ and $g_r(\mathbf{x}, t) = \nabla_{u_r} \mathcal{J}$ are given by the Frechét derivatives of the objective function with respect to the background wavefields. The double dots represent the second derivative with respect to time.

The gradient $\nabla_m \mathcal{J}$ indicates which parts of the model must change in order to reduce the mismatch between the baseline and monitor migrated images. Inversion locates the areas in the model that experience a perturbation in physical parameters induced by the reservoir production.

RESERVOIR DEPLETION MODEL

When a reservoir is produced, the depletion causes geomechanical effects both inside and outside the reservoir. Because of the drop in pore pressure, the reservoir rock compacts and the effective stress (and seismic velocity) increases; outside the reservoir the rock is strained and the seismic velocity decreases. This observed phenomenon can be analyzed using time-shifts (Hatchell and Bourne, 2005; Hale et al., 2008; Smith and Tsvankin, 2012) and describes the complex changes in subsurface stress conditions caused by oil and gas production.

In order to test our velocity estimation procedure in a more realistic scenario, we use a geomechanical model designed by Smith and Tsvankin (2012) to obtain the model parameters for a reservoir under depletion. We generate data with acoustic finite-differences using density reflectors at various depths and with absorbing boundary conditions on each side of the model (Figure 1(a)). The initial velocity model is homogenous and equal to 2.07 km/s velocity. Figure **??** shows the model of the reservoir undergoing a 15% depletion. Observe the complex pattern of the velocity anomaly outside the reservoir. The perturbation is positive inside the reservoir because of compaction, negative outside the reservoir because of strain, and has positive sidelobes on both sides of the model. The velocity model perturbation inside the reservoir is about +15% with respect to the baseline model. Figure 2 shows the data obtained for the baseline and monitor surveys. Observe the internal multiples arriving after 2.5 s and following the strong

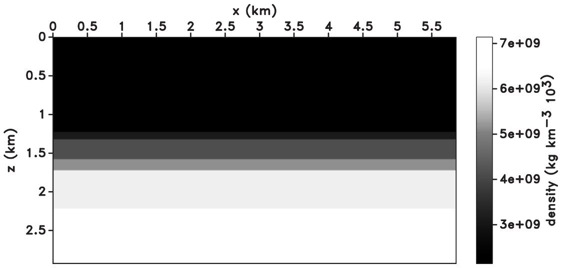

(a)

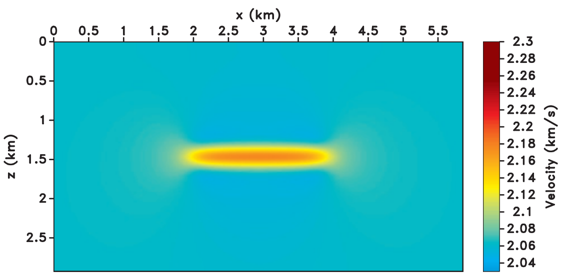

(b)

Figure 1: (a) Density model used to simulate the reflecting interfaces. (b) Velocity model of the depleted reservoir. The original model is homogenous with 2.07 km/s velocity. Observe the characteristic shape of the anomaly with increasing velocity inside the reservoir (because of compaction) and decreasing velocity outside the reservoir (because of strain).

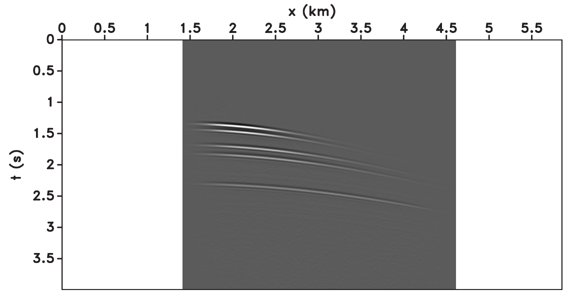

(a)

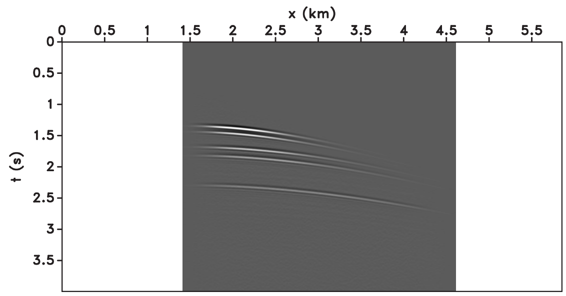

(b)

Figure 2: (a) Baseline data and (b) monitor data simulated in the depleted reservoir. By inspection, it is impossible to observe any perturbation in the arrival times.

deeper reflection. From visual inspection, it is difficult to notice any shift in the waveform. However, because of the opposite sign of the velocity anomaly, the early arrivals (around 1.2 s) are delayed and the late waveforms (after 1.5 s) are advanced in time.

Our inversion experiment uses a single shot gather with the source located at $x = 1.5$ km and with a streamer 3.2 km long. The length of the cable is about the same as the lateral extent of the reservoir. The streamer carries 300 evenly spaced receivers and the receiver spacing is 8 m. The gradient of the objective function is smoothed using a triangular filter with radius 2 samples vertically and 5 samples horizontally. The model is updated using a steepest descent algorithm. We implement regularization through triangular smoothing. The smoothing procedure acts as regularization in the inversion by removing spurious high wavenumber sidelobes in the gradient. More sophisticated and structure oriented regularization approaches can be used for more complex subsurface scenarios.

Figure **??** shows the true perturbation, the inverted perturbation after 30 iterations, and the result of our single-shot inversion after 60 tomographic iterations. Because of the limited aperture of the acquired data, the wavefields are not sensitive to the complete extent of the anomaly. Nonetheless, the imaged portion of the model allows us to constrain the size and location of the anomaly. Notice that the inversion is able to recover the weaker perturbation outside the reservoir of opposite sign with respect to the perturbation within the reservoir, and observe that we are also able to correctly image the left side of the anomaly thus correctly constraining its lateral extent. After 30 iterations we are already able to locate and constrain the anomaly, but the amplitude is far from the correct value. Increasing the number of iterations, the value of the perturbation builds up and better approximates the correct value.

Figure 4 shows the shifts between the baseline and monitor migrated images before inversion, after 30, and after 60 tomographic iterations. Black indicated a downward shift whereas white indicate an upward shift. Before inversion the shallower and deeper reflectors are shifted in opposite direction because of the different sign of the anomaly inside and outside the reservoir (see Figure **??**). By observing Figure 4(a), we see that the shallower reflector is sensitive to both signs of the anomaly and the leftmost imaged part of the reflector is shifted down (black) while the rightmost part is shifted up (white). After 30 iterations most of the shifts between the two images is already corrected (Figure 4(b)). After inversion the reflectors are better aligned and the shifts for all reflectors approach zero (Figure 4(c)). Inversion warps the monitor image into the baseline image and returns the velocity anomaly that corrects the shifts of the im-

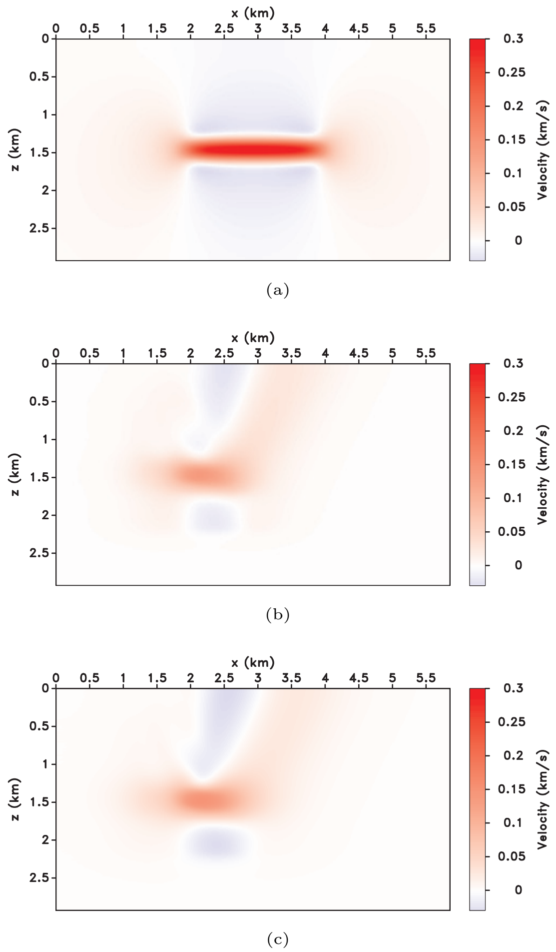

Figure 3: (a) Real time-lapse model perturbation, (b) inverted perturnarbation after 30 iterations, and (c) inverted perturbation after 60 iterations of wavefield tomography. Notice that we are able to correctly image the anomaly and also constrain its lateral extent at about $x = 2$ km.

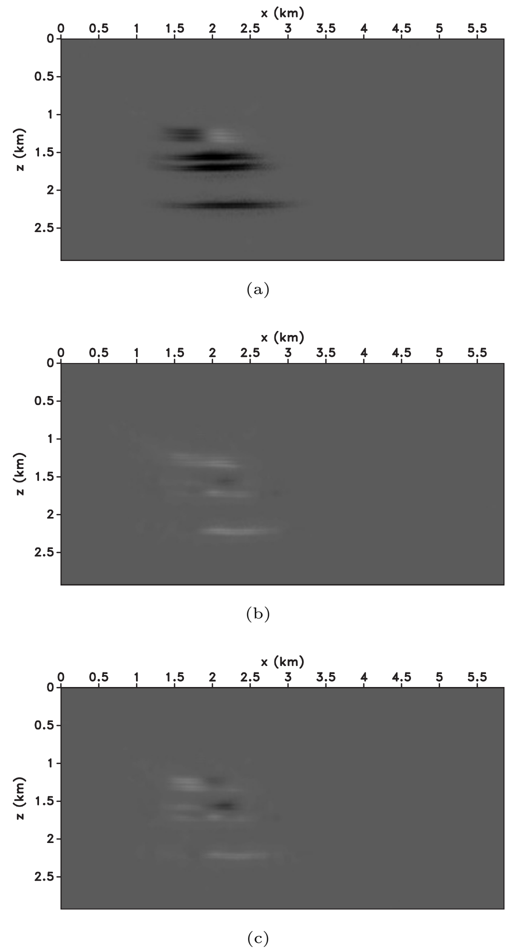

Figure 4: (a) Initial estimated shifts, (b) shifts after 30 iterations, and (c) estimated shifts after 60 iterations of wavefield tomography. Black indicates positive (downward) shifts and white represents negative (upward) shifts. Inversion matches the baseline and monitor images and reduces the shifts between them.

aged interfaces. By further increasing the number of iterations, we do not consequently decrease the objective function but instead we better recover the value of the perturbation.

CONCLUSIONS

Local correlations in the image domain allow us to assess the quality of the velocity model from a limited number of migrated images. In 4D seismic applications, we can quickly estimate a perturbation in the migration model by comparing shot images from the baseline and monitor surveys. In the image domain, we measure the consistency and similarity of locally coherent events, like the local dip of the reflectors; these features are weakly sensitive to differences in the acquisition geometry and make our approach more robust against repeatability issues in the survey as compared to strategies in the data domain. The method is able to recover the relative error in the model and does not require separate velocity analysis steps for baseline and monitor survey in order to estimate the differences between the two models.

ACKNOWLEDGMENTS

We would like to thank Jyoti Behura of Colorado School of Mines for interesting discussions about 4D time-lapse seismic and for encouraging FP to look into this problem. This work was supported by the sponsors of the Consortium Project on Seismic Inverse Methods for Complex Structures. The reproducible numerical examples in this paper use the Madagascar open-source software package freely available from http://www.ahay.org and the Mines JTK freely available at https://github.com/dhale/jtk.

Time-lapse tomography using apparent image displacements

REFERENCES

Aki, K., and P. G. Richards, 2002, Quantitative seismology: University Science Books.

Fichtner, A., H.-P. Bunge, and H.Igel, 2006, The adjoint method in seismology I. theory: Physics of the Earth and Planetary Interiors, 86–104.

Hale, D., 2007, A method for estimating apparent displacement vectors from time-lapse seismic data: Technical Report CWP-566, Center for Wave Phenomena, Colorado School of Mines.

Hale, D., B. Cox, and P. J. Hatchell, 2008, Apparent horizontal displacements in time-lapse seismic images: Presented at the SEG Technical Program Expanded Abstracts, SEG.

Hatchell, P. J., and S. J. Bourne, 2005, Measuring reservoir compaction using time-lapse timeshifts: Presented at the 75th Ann. Internat. Mtg., Soc. of Expl. Geophys.

Lumley, D. E., 2001, Time-lapse seismic reservoir monitoring: Geophysics, **66**, 50–53.

Perrone, F., and P. Sava, 2012, Wavefield tomography based on local image correlation: Presented at the 74th Conference and Exhibition, EAGE.

Plessix, R.-E., 2006, A review of the adjoint-state method for computing the gradient of a functional with geophysical applications: Geophys. J. Int., **167**, 495–503.

Rickett, J. E., and D. E. Lumley, 2001, Cross-equalization data processing for time-lapse seismic reservoir monitoring: A case study from the Gulf of Mexico: Geophysics, **66**.

Sava, P., and B. Biondi, 2004, Wave-equation migration velocity analysis. I. Theory: Geophysical Prospecting, **52**, 593–606.

Shragge, J. C., and D. E. Lumley, 2012, 4D seismic wave-equation depth migration velocity analysis: Presented at the 74th Conference and Exhibition, EAGE.

Shragge, J. C., T. Yang, and P. Sava, 2012, Time-lapse image-domain velocity analysis using adjoint-state methods: Presented at the SEG Technical Program Expanded Abstracts, Soc. of Expl. Geophys.

Smith, S. S., and I. Tsvankin, 2012, Modeling and analysis of compaction-induced traveltime shifts for multicomponent seismic data: Geophysics, **77**, T221–T237.

Yang, T., and P. Sava, 2011, Image-domain waveform tomography with two-way wave-equation: Presented at the 81th Ann. Internat. Mtg., Soc. of Expl. Geophys.

———, 2012, Illumination compensation for image-domain wavefield tomography: Presented at the 74th Conference and Exhibition, EAGE.